# Acoustic evidence for seasonal resource-tracking migration by a top predator of the deep sea

William K. Oestreich[a,*], Kelly J. Benoit-Bird[a], Briana Abrahms[b], Tetyana Margolina[c], John E. Joseph[c], Yanwu Zhang[a], Carlos A. Rueda[a], John P. Ryan[a]

[a] Monterey Bay Aquarium Research Institute, Moss Landing, CA 95039, USA

[b] Center for Ecosystem Sentinels, Department of Biology, University of Washington, Seattle, WA 98195, USA

[c] Naval Postgraduate School, Monterey, CA 93943, USA

*Corresponding author: William K. Oestreich

**Email:** woestreich.research@gmail.com

**Author Contributions:** W.K.O., K.J.B., and J.P.R. conceived the study; W.K.O., K.J.B., and J.P.R. designed the research; J.P.R. collected data; W.K.O., B.A., T.M., Y.Z., C.A.R., and J.P.R. developed methods; W.K.O., T.M., and J.P.R. performed analyses; and W.K.O. wrote the manuscript with contributions from all authors.

**Competing Interest Statement:** The authors declare no competing interests.

**Keywords:** phenology, deep sea, movement ecology, bioacoustics, resource tracking

**Abstract**

The strategies that animals employ to track resources through space and time are central to their ecology and ability to adapt to environmental variation. These spatiotemporal movement patterns also reflect underlying ecosystem phenology. In ecosystems influenced by seasonal variation in solar angle, the fitness of diverse taxa depends on seasonal movements to track resources along latitudinal or elevational gradients. Deep pelagic ecosystems, where sunlight is extremely limited or entirely absent, represent Earth's largest habitable space and yet ecosystem phenology and effective animal movement strategies in these systems are unknown. Here, we combine long-term passive acoustic monitoring data with animal movement simulations to test a suite of movement strategies for foraging predators in the deep pelagic. Examining more than seven years of acoustic data in the Central California Current System (CCCS), we find evidence for seasonal, latitudinal migratory movements in a deep pelagic top predator, the sperm whale (*Physeter macrocephalus*). Our analyses reveal seasonal and interannual variability in the presence of foraging whales in the CCCS. Importantly, while these highly-mobile predators of the deep are often described as nomadic, integration of population-level acoustic observations with simulations of individual-level movement instead provides first evidence that this sperm whale population undertakes a seasonal resource-tracking migration. These findings improve understanding of the drivers and flexibility of long-distance movements in this cryptic predator inhabiting a difficult-to-observe ecosystem. More broadly, these migratory movement patterns indicate previously unknown environmental seasonality at depth, thus shedding light on the shrouded phenology of deep pelagic ecosystems.

**Significance Statement**

Animal movements to track resources in space and time reflect underlying ecosystem dynamics. In the deep ocean, both ecosystem phenology and the movement strategies that highly-mobile animals employ remain murky due to the challenge of persistent observation. By combining 7-plus years of continuous acoustic recordings with movement simulations for sperm whales, we find that these deep ocean top predators employ a seasonal resource-tracking migration strategy often displayed by terrestrial and surface ocean animals. Our findings reveal a previously unknown movement strategy in a cryptic deep ocean predator, and provide insight on the ability of this endangered species to respond flexibly to environmental perturbations. Finally, results indicate that deep ocean ecosystems likely exhibit greater seasonal-latitudinal variability than previously appreciated.

## Main Text

### Introduction

The movement strategies that animals use to track resources in space and time drive many aspects of their ecology, mediate their ability to respond to environmental perturbations, and provide insight into the spatiotemporal dynamics of the ecosystems they inhabit (1). These individual and group-level movement strategies typically result from spatiotemporal patterns of resource availability (2), and manifest in distinct patterns of population-level distribution in space and time (3). For example, nomadic resource tracking has evolved in aseasonal and unpredictable environments, leading to irregular patterns of individual movement and population distribution (4). Conversely, in seasonal ecosystems that display spatiotemporal resource dynamics driven by seasonal variation in solar angle, many species have evolved to undertake seasonal migrations (4).

Resource-tracking migrations represent an important connection between ecosystem dynamics and animal movement, closely linking ecosystem phenology with that of seasonal animal migrations (1, 5). Under this strategy, migrating animals may maximize their resource gain by tracking resource phenology as it propagates across spatiotemporal gradients such as latitudes or elevations (6). Such resource tracking has been shown to provide a number of individual and population-level benefits, from enabling animals to have more prolonged access to food (7), to increasing fat gain (8) and allowing migratory populations to have higher growth rates than sedentary populations (9). These linkages between resource dynamics and animal movement strategies are increasingly well-understood in seasonal terrestrial (2, 5, 8, 10), freshwater (11), coastal marine (12), and epipelagic (13–18) ecosystems across the globe.

Few studies to-date have assessed these connections between ecosystem dynamics and animal movement in Earth's largest habitable space: deep pelagic ecosystems. These oceanic waters deeper than 200m, where little sunlight penetrates, are often characterized as stable, resource-scarce, and poorly-understood (19). This view of stability has historically included a lack of seasonality in ecosystem dynamics. More recently, a growing body of evidence suggests elements of seasonality (albeit dampened (19)) in both biological and physical processes in the deep ocean (20–24). Limited understanding of deep ocean phenology, particularly for highly-mobile and high-trophic-level animals, is underpinned by the challenge of making continuous and detailed observations in these ecosystems (19). Given the global extent, high endemic biodiversity, and major role in global biogeochemical cycles of deep pelagic ecosystems, understanding the phenology of these ecosystems and the evolved movement strategies of their inhabitants is important to advance fundamental ecology and inform ecosystem management.

We address this gap by integrating long-term passive acoustic monitoring data and movement simulations for a deep pelagic top predator, the sperm whale (*Physeter macrocephalus*). Sperm whales are a deep-diving oceanic predator, diving to depths of hundreds-to-thousands of meters (25) to forage on diverse deep pelagic prey (26). Thus, studying the movement patterns of these ocean giants can provide a rare window into the phenology of the deep ocean environment. In addition, sperm whales produce the loudest known biological sounds (27) which not only reveal the presence of this often-cryptic species over large ocean volumes, but also transmit rich behavioral and demographic information about detected individuals. Echolocation clicks are central to the foraging ecology of sperm whales in the low-light conditions of the deep ocean, and further indicate individuals' behavioral state (foraging), size (both inter-click-interval (28) and inter-pulse-interval within individual clicks (29) correlate with size), and sex and age-class (sperm whales are sexually dimorphic, with males being much larger (30)). Sperm whales use echolocation in both the meso- and bathypelagic (31) to locate a variety of squid and fish prey species (26). As a result, monitoring patterns of sperm whale echolocation click detection can provide insight into the phenology of both this top predator and the deep pelagic ecosystems in which they forage.

In the Northeast Pacific (Figure 1A), foraging sperm whales have been detected acoustically year-round, specifically in the Gulf of Alaska (GoA) (32, 33). Individuals of this

population have expansive home ranges, exhibiting wide-ranging movements which include travel between the GoA and the Central California Current System (CCCS; Figure 1A) (34–36). Yet the regularity, seasonality, and behavioral context of such movements have historically remained unclear. Previous studies have indicated that latitudinal movements are likely irregular, resulting from aseasonal nomadic movements (34, 35) consistent with the canonical view of dampened (or nonexistent) seasonality in the deep sea (19). Yet previous acoustic studies in the GoA have suggested seasonality in foraging sperm whales' presence (32, 33), challenging the assumption of aseasonal nomadic movements. Others have suggested that long-distance latitudinal movements represent migration between distinct high-latitude foraging and low-latitude breeding habitats (37), akin to the seasonal migrations of many baleen whales. Partial migration (with only adult males undertaking these movements) has also been suggested (30), yet multiple sexes and age classes have been observed in both the GoA (35) and CCCS (36, 38). As with most inhabitants of deep pelagic ecosystems, this murky understanding of sperm whales' movement strategies arises from the challenge of observing their behavior persistently at sufficient scale (39, 40) and limited understanding of phenology in their foraging habitat.

Here, we investigate the strategies underlying movements of this deep pelagic top predator in the Northeast Pacific. We consider the often-assumed strategy of nomadism in sperm whales alongside three additional hypothesized movement strategies: seasonal migration between distinct habitats, partial migration, and seasonal resource-tracking migration. We test these hypotheses by first applying automated acoustic detection methods to more than seven years of passive acoustic recordings in order to discern seasonal and interannual patterns of foraging sperm whale presence in the CCCS as compared to the GoA. Passive acoustic monitoring approaches provide a valuable lens to assess population-level animal distributions and behavior (41), particularly in largely-inaccessible oceanic ecosystems (17, 42) and in cases where information beyond presence alone (e.g., behavioral state) can be discerned from the properties of detected acoustic signals (43). We then integrate these empirical patterns with simulations of individual-level movement driven by each of the hypothesized movement strategies. Hypothesis-testing using this integrated approach allows us to (*i*) determine the unknown seasonality and regularity of foraging sperm whale presence in the CCCS, (*ii*) evaluate the individual-level strategies underlying sperm whales' wide-ranging foraging movements in the deep ocean, and (*iii*) consider the seasonal and interannual flexibility afforded by these movement strategies in the context of rapid environmental change.

## Results

Acoustic detection revealed year-round, seasonally-varying presence of foraging sperm whales in the CCCS (Figure 2). The frequency of foraging sperm whale presence in the average annual cycle reached a maximum in January (mean of 59.3% of days present) and a minimum in July (mean of 31.1% of days present). Monthly percent of days with foraging sperm whale presence is a useful metric in this context for multiple reasons: (1) it provides sufficient temporal resolution to assess seasonal trends, the primary timescale of focus in this study; (2) automated detector performance is very high at daily resolution (Figure S1), providing high confidence in this metric; and (3) this metric matches that used in previous studies of foraging sperm whale presence elsewhere in the Northeast Pacific (32, 33), allowing for direct comparison of seasonal presence of foraging whales across latitudes. June – September had a significantly lower mean percent of days with presence as compared to the January maximum, and November – April had a significantly higher mean percent of days with presence as compared to the July minimum (Figure 2B). A generalized additive model (GAM) revealed a significant relationship between monthly percent of days with presence and month, with year nested as a random effect ($p < 0.001$; 45.4% deviance explained; Figure S2), further indicating seasonality in foraging sperm whale presence in the CCCS. Detection seasonality did not result from seasonal changes in ambient noise or maximum detection range. Maximum click detection range was slightly greater during the summer minimum in click detections relative to detection range during the winter detection maximum (Figure S3),

suggesting that the degree of seasonality shown here (Figure 2B) is a conservative estimate. Interannually, the percent of recording days on which foraging sperm whales were detected varied little, with the exception of 2016 (Figure 2A). Foraging sperm whales were detected on 63.4% of recording days in 2016, whereas the percentage in all other years varied between 38.6-49.9%.

Simulations of individual-level movement (Figure 3) yielded qualitatively and quantitatively-distinct patterns in the seasonal-latitudinal distribution (Figure 3) and seasonal acoustic detection (Figure 4) of agents, dependent on the movement strategy employed. The simulation of seasonal resource tracking agents yielded year-round presence with moderate seasonality at both southern and northern listening ranges (Figure 3A), peaking in the winter and summer for the southern and northern listening ranges, respectively (Figure 4B). The seasonal patterns of acoustic detection arising from seasonal resource-tracking migration represented the only simulated results matching the defining qualities of empirically-observed patterns: year-round presence with substantial and opposite seasonality at both higher and lower-latitude listening ranges (Figure 4). Agents following nomadic resource tracking decision rules showed no seasonality in detection at northern or southern listening ranges (Figure 4B), driven by similar winter and summer latitudinal distributions (Figure 3B). Agents undertaking seasonal migrations between distinct habitats showed strong and opposite seasonality in latitudinal distribution (Figure 3C). This simulation yielded high levels of detection during winter and zero detections during summer at the southern listening range, while the northern listening range showed high levels of detection during summer and zero detections during winter (Figure 4B). Simulation of partial migration resulted in strong seasonality in detection at the northern listening range (high levels of detection in summer, zero detections in winter) and year-round detection with weak seasonality at the southern listening range (Figure 3D; Figure 4B).

Simulated acoustic detection patterns for seasonal resource-tracking migration were also quantitatively most similar to empirical acoustic detection, yielding a root-mean-square deviation among monthly means of only 15.6% (Figure 4B). All other simulated movement strategies resulted in greater deviance from empirical observations in monthly acoustic detections (22.4% for nomadic resource tracking, 31.7% for seasonal migration between distinct habitats, 31.9% for partial migration, Figure 4B).

## Discussion

Animals' movement strategies shape their ecology and their ability to respond to environmental perturbations. Moreover, these strategies offer a window into revealing the spatiotemporal dynamics of the ecosystems they inhabit (1). Our findings provide the first evidence for seasonal resource-tracking movements by a top predator in the deep ocean, the sperm whale, suggesting seasonal-latitudinal phenological patterns in the meso- and bathypelagic prey on which sperm whales forage. These results shed light on the strategy underlying this cryptic top predator's long-distance movements, flexibility in this endangered species' foraging and movement behaviors in response to environmental perturbations, and the phenology of the poorly-understood deep ocean ecosystems in which they forage.

The long-term acoustic results presented here indicate clear seasonality in the latitudinal movements of foraging sperm whales, with greater frequency of echolocation click detection in the CCCS during winter (Figure 2B; Figure S2), opposite the known summer peak of detection in the GoA (32, 33) (Figure 4A). Despite this opposite seasonality, foraging sperm whales are detected year-round in both locations. We posit that these patterns indicate a seasonal resource-tracking migration in this population, based on several lines of evidence. First, seasonal resource-tracking migration is the only hypothesized movement strategy allowing for both year-round presence and significant seasonality in presence across latitudes (Figure 3A; Figure 4B), matching empirical observations (Figure 4A). Nomadism yields relatively uniform latitudinal distributions and year-round but non-seasonal acoustic detection (Figure 3B; Figure 4B). Seasonal migration between distinct habitats (Figure 3C; Figure 4B) leads to seasonality in acoustic detection, but does not allow for year-round detection across latitudes. Partial migration similarly does not allow for year-round detection across latitudes, and only results in significant

seasonality at some latitudes (Figure 3D; Figure 4B). Additionally, if partial migration were occurring, we would expect the migratory demographic (previously hypothesized to be adult males, with larger body sizes and higher inter-click-intervals (ICI)) to drive seasonality in ICI matching that of percent presence. Yet we do not observe clear seasonality in ICI in the CCCS and also find no relationship between ICI and percent presence (Figure S4), further refuting the possibility that seasonality in acoustic detection is driven by partial migration between distinct habitats in this sexually-dimorphic population. Finally, the results presented here and previously (32, 33) specifically document the presence of foraging (echolocating) individuals, underscoring that sperm whales are actively foraging in these study locations and are not only present for non-foraging behaviors (e.g., mating).

This discovery of resource-tracking migratory movements has implications for understanding this deep ocean predator's fundamental ecology and ability to adapt to rapid environmental change. Seasonal resource-tracking migrations in terrestrial and epipelagic populations typically evolve as a strategy to maximize resource gain in dynamic, seasonal ecosystems (1, 4, 8). Variability around the average seasonal-latitudinal patterns exhibited by foraging sperm whales (Figure 2) suggests that the cues driving their latitudinal movements are not fixed seasonal cues (e.g., day length), affording flexibility to respond to environmental variation and change. More specifically, sperm whales were most often detected in the CCCS during 2016 (Figure 2A), a year in which a persistent marine heatwave combined with a strong El Niño to drive widespread biological impacts in both the CCCS (44) and GoA (45). By exhibiting a movement strategy driven by resource tracking rather than fidelity to a fixed foraging area or migratory schedule, sperm whales appear to respond flexibly to interannual variability in oceanographic conditions (Figure 2A; (46)). Such flexibility is often characteristic of greater resilience to environmental perturbations (47) including marine heatwaves (48). Understanding the individual and population-level outcomes of such flexibility in this sperm whale population remains an important and rich area for future study.

While the specific cues that enable this seasonal resource-tracking migration remain unclear, some combination of individual and social information likely influences these movements. As air-breathing predators, sperm whales spend significant time in surface waters subject to seasonal variability in solar irradiation. This provides a direct means of tracking progression of the seasons, perhaps enabling movements influenced by spatiotemporal memory similar to that observed in highly-mobile epipelagic predators (16). Further, sperm whales and other deep-foraging odontocetes are known to plan deep foraging dives from near the surface using long-range echolocation (25, 49). Given that mesopelagic and bathypelagic prey can display significant heterogeneity in density (50), this approach might allow sperm whales to minimize diving effort in areas of low prey density and allot greater time and energy to horizontal movements to track seasonal-latitudinal forage variability. Because sperm whales echolocate to find prey, long-distance acoustic information on the foraging behavior of conspecifics might further direct this search, similar to the "mobile sensory networks" formed by echolocating bats (51). Social learning of foraging and movement strategies could also play a role (52, 53), as sperm whales are highly-social animals (30).

More broadly, because animal movements evolve to reflect underlying resource dynamics in the ecosystems they inhabit, our findings indicate seasonal-latitudinal variability in elements of the deep pelagic ecosystems in which sperm whales forage. This challenges the view of seasonal stability in the deep ocean, and contributes to a growing body of evidence for seasonal dynamics in these ecosystems (20–24). Given that little if any sunlight penetrates to the depths at which sperm whales forage, it is unlikely that this seasonality in the deep ocean is driven by direct seasonal changes in primary productivity. Instead, this seasonality likely arises indirectly via interactions between surface and deep waters. For example, diel vertical migration of animals between the meso- and epipelagic can vary seasonally in terms of depth distribution of animals, migration distance, total biomass, and carbon transport (21, 54, 55). In Monterey Bay specifically, total biomass throughout the meso- and epipelagic is at a minimum in spring and summer, rises in the fall, and remains elevated through the winter (21), allowing for greater transport of biomass between surface and deep waters during the seasons when foraging sperm

whale detections peak in this region (Figure 2B). Many of the sperm whale's primary prey are themselves vertical migrators (31), providing an even more direct link between seasonal processes in the surface ocean and the seasonal-latitude resource tracking in sperm whales documented here.

Taken together, our findings not only reveal unexpected seasonal resource-tracking by a top predator in the deep ocean, but also point toward previously underappreciated seasonal variation in light-limited deep pelagic ecosystems. This study underscores the need for additional research to enhance both fundamental and applied ecology on the phenology of deep pelagic ecosystems across trophic levels. A growing suite of technologies, including remotely-operated vehicles, autonomous underwater vehicles, and continuous active and passive acoustic monitoring are providing an unprecedented opportunity to observe and understand deep ocean ecosystems (19, 20, 56). Especially when integrated (20, 57), these tools can continue to shed light on our murky understanding of seasonal processes and animals' resource-tracking strategies in the deep sea. In turn, we can provide more precise scientific insight in support of spatiotemporally dynamic ecosystem management efforts which have to-date been used on land and in the surface ocean (58), but which may be possible and valuable in open and deep ocean ecosystems (59).

## Materials and Methods

*Study site and hydrophone recordings*

Acoustic recordings were collected on the continental slope outside Monterey Bay, CA, via icListen hydrophones sequentially deployed on the Monterey Accelerated Research System (MARS) cabled observatory (36° 42.75'N, 122° 11.21'W; depth 891 m). These hydrophones recorded at 256kHz; all recordings were decimated (60) to a sample rate of 16 kHz before analysis to dramatically reduce the computational time required to run the workflow described below. While directional components of sperm whale echolocation clicks can have a peak frequency exceeding the Nyquist frequency of these 16kHz audio files (27), this sample rate allows for reliable detection of the omnidirectional low-frequency component of these clicks. Previously, these clicks have been reliably detected in audio files with a sample rate as low as 1kHz (32).

*Passive acoustic analyses*

Sperm whales produce a variety of click types associated with distinct behaviors. The present analysis focused only on "usual" clicks, which are associated with searching for prey (30) and are hereafter referred to as clicks. We used a two-step automated workflow (detection and filtration) to determine presence or absence of sperm whale clicks at daily resolution. Candidate detections of individual clicks were generated using a band limited energy detection (BLED) approach implemented in Raven Pro v1.6. The BLED "estimates the background noise of a signal and uses this to find sections of signal that exceed a user-specified signal-to-noise ratio threshold in a specific frequency band, during a specific time" (61). We manually tuned the parameters of a BLED (Table S1) to maximize the chances of detecting sperm whale clicks under a range of background noise scenarios, but this coarse first step in acoustic processing also generated many false positives.

These false positives were filtered out in the second step of our automated workflow by searching BLED results for repetitive, evenly-spaced sequences of detections matching the known inter-click interval (ICI) of sperm whale usual clicks (~0.5 – 2.0 seconds (62)). Because the intervals between clicks in sperm whale echolocation sequences are largely regular but not exactly constant, we calculated the time difference between each BLED detection (inter-detection interval; IDI), then rounded to the nearest quarter second to enable a search for sequences of detections with a near-constant IDI. Using these rounded IDI values, each day of recording was automatically searched for IDI sequences matching three criteria: (1) rounded IDI must be between 0.5 and 2.0 seconds (inclusive); (2) rounded IDI must be constant; and (3) the number of

consecutive IDI values meeting criteria (1) and (2) must meet a sufficient number of repetitions (r) to confidently determine sperm whale echolocation click presence. We considered any day with at least one sequence meeting these criteria to have sperm whale clicks present; any day without any sequence meeting these criteria was considered to have such clicks absent. Setting the number of repetitions required (r) to consider clicks present can significantly impact the accuracy of this automated workflow at daily resolution (Figure S1). The optimal value for this parameter was determined via comparison to manual identification of sperm whale search clicks. Manual assessments were completed for one randomly chosen day of each month in both 2016 and 2020, as well as two days of known sperm whale presence near our recording location (Figure 1) in late 2022. These 26 days provided a representative range of soundscape conditions by covering the full seasonal cycle, including periods recorded by each of the two consecutively-deployed hydrophones, and including recording periods both affected (2020) and unaffected (2016) by the change in anthropogenic noise conditions associated with the COVID-19 pandemic (63). We found optimal performance at r = 6, yielding a daily balanced accuracy of 97% (precision = 100%, recall = 94%) and false positive rate of 0% (Figure S1).

Using this time series of daily-resolution presence and absence, we then calculated monthly and annual percent of recording days with foraging sperm whales present for each year and month of the time series. This monthly percent presence metric matches the metric used in previous passive acoustic studies on sperm whale echolocation at Ocean Station PAPA in the Gulf of Alaska over the years 1999-2001 (32) and 2007-2012 (33). Monthly percent presence values were estimated graphically from these studies and were later used in comparison to simulation results (Figure 4A; see below).

Seasonality in the detection of foraging sperm whales in the CCCS was assessed statistically in two ways. First, we used t-tests to identify months with mean detection rates significantly higher or lower than the maximum (January) and minimum (July) monthly means (Figure 2). Second, we constructed a generalized additive model of monthly percent presence as a function of month with year nested as a random effect to test for the deviance in percent presence explained by the seasonal cycle alone (Figure S2). Finally, we calculated the ICI of all detected click sequences in the time series, allowing for comparisons of ICI to month and monthly percent of recording days with foraging sperm whales present (Figure S4).

*Estimation of ambient noise levels, acoustic propagation loss, and detection range*

To assess seasonality in click detection range at MARS, we evaluated seasonality in both ambient noise levels and acoustic propagation loss between sound source and acoustic receiver. The ambient noise level metric is single-sided mean-square sound pressure spectral density, following ISO 18405 3.1.3.13 (ISO, 2017). From daily files of 16 kHz audio data spanning the full study period, daily mean noise levels were computed for the frequency band targeted by the click detector, 1.4 to 4 kHz. Daily values were binned by month across years to examine seasonality (Figure S3B).

Acoustic propagation loss was modeled for a sound source matching the characteristics of sperm whale echolocation at the frequencies targeted by our automated detection approach. Specifically, we modeled transmission loss for an impulsive sound source at 2.7kHz (the center frequency of the BLED), 185 dB re: 1μPa at 1m (peak level of the omnidirectional low-frequency component of sperm whale echolocation clicks (64)), and source depths of 100, 500 and 1000m (typical of echolocation in foraging sperm whales in many ecosystems (25, 31, 64, 65)), received at the location of MARS. Propagation loss was modeled for January and July to assess seasonality in click detection range. Oceanographic water column properties for the January and July model runs were calculated as the climatological mean of oceanographic conditions over the period 2016-2022 as estimated by the HYCOM (HYbrid Coordinate Ocean Model) data assimilative system (66) with 4.8 minute spatial resolution. Acoustic propagation loss was then calculated for each of 360 1° bearings from MARS using a wave-theory parabolic equation model that accounts for absorption in both the water column and the bottom, scattering in the water column and at the surface and bottom, geometric spreading (spherical and cylindrical), refraction, and diffraction (67). Finally, detection range for each source depth and season was estimated for

each of these 360 bearings, requiring received level at MARS to exceed 5.0 dB (SNR of the click detector, Table S1) above monthly median ambient noise levels (Figure S3).

*Simulation of individual-level movement strategies*

To test hypotheses regarding the individual-level movement strategies underlying empirically observed patterns of sperm whale foraging, we employed simulations in which agents move through a spatial domain (Figure 3) with two hydrophone "listening ranges" (one at higher latitude and one at lower latitude), analogous to passive acoustic monitoring of sperm whales in the Gulf of Alaska (32, 33) and the Central California Current System (present study). In all simulations, 100 agents moved daily according to strategy-specific decisions over a ten-year period. The spatial domain in which these simulations occur is not meant to specifically represent the spatial dimensions of the North Pacific or hydrophone listening ranges used in the present or previous studies. Instead, this spatial domain provides a simplified arena for testing realistic individual movement strategies (68) and their influence on population-level spatiotemporal patterns of acoustic detection. Agent step lengths, hydrophone listening ranges, and domain dimensions were scaled proportionally to allow agents to move seasonally without leaving the domain, while also having limited probability of acoustic detection even if present at the latitude of a listening range (i.e., listening ranges cover only a proportion of both the latitudinal and longitudinal dimensions). This approach allows for realistic probabilities of acoustic detection for a large number of individual position-days (365,000 per simulation) without the extreme computational expense of simulating a number of agents comparable to the estimated population size of sperm whales in the eastern North Pacific (~2000 (69)).

We used known information about the typical step lengths, turn angles, and seasonality of movement for well-documented movement "syndromes" (68) to formulate movement decision rules (described below) for agents representing four distinct movement strategies: nomadic resource tracking, seasonal migration between distinct habitats, partial migration, and seasonal resource-tracking migration. We explored the population-level acoustic detection patterns resulting from each of these four movement strategies via four separate simulations with agents subject to these decision rules. At each daily timestep of each ten-year simulation, we recorded each agent's position and presence or absence in each of the simulated hydrophone listening ranges. The population-level patterns resulting from each simulation were compared to empirical observations of seasonality in sperm whale foraging (Figure 4A) in the Gulf of Alaska (32, 33)(32, 33) and the Central California Current System (present study; Figure 2B). Specifically, we calculated the root-mean-square deviation of simulated monthly mean acoustic detection results from both listening ranges relative to empirical results from the Gulf of Alaska and the Central California Current System. All results in Figure 4B show agent position and acoustic detection statistics for years 2-10 of the simulation to minimize the influence of initial conditions.

We simulated nomadic individuals using decision rules previously documented for nomads (68): low probability of behavioral state switching between active foraging and searching, small step lengths and uniformly-distributed turn angles during active foraging, and longer step lengths during searching with normally-distributed turn angles (around the initial direction after switching from foraging to searching).

We simulated migration between distinct habitats again using the decision rules documented by (68): four months of foraging in a southern range (steps defined by uniform step length and turn angle distributions), two months of northward migration (longer step lengths and normal turn angle distribution centered on north), four months of foraging in a northern range (steps again defined by uniform step length and turn angle distributions), and finally two months of southward migration (longer step lengths and normal turn angle distribution centered on south).

We simulated partial migration by assigning 50% of agents to a migratory group and 50% of agents to a resident group. Migrants followed the decision rules described above for migration between distinct habitats; residents followed the decisions rules described above for nomadic resource tracking, but only in the southern portion of the simulation domain.

We simulated movements to track resources with a shifting seasonal-latitudinal distribution using decision rules similar to that for nomadic resource tracking as described above,

but with differences in movement behavior between times and locations of active foraging. Rather than searching in a single direction with turn angles normally-distributed around a randomly-selected initial search direction (as in nomads), agents in this simulation moved between active foraging periods by tracking resources with headings normally-distributed around due north and due south. The probability of northward-centered or southward-centered heading distributions during resource tracking varied seasonally to mimic seasonal shifts in latitudinal forage availability.

*Software*

All analyses and visualizations of click detections and individual-level movement strategies were conducted in R version 4.2.0 (70). The map in Figure 1A was created using the R packages "ggOceanMaps" (71) and "geosphere" (72). Background noise and acoustic propagation analyses were conducted in Matlab (73). Candidate click detections were generated using Raven Pro v1.6 (61).

*Data and code availability*

Raw (256 kHz) and decimated (16 kHz) acoustic data from the MARS hydrophone are available here: https://docs.mbari.org/pacific-sound/ (74). Code for processing acoustic data, analyzing sperm whale detections, and simulating individual-level movement strategies are available here: https://github.com/woestreich/cachalot_seasonal (75).

## Acknowledgments

Thank you to Melissa Chapman and Megan McKenna for discussions which improved this manuscript. This research was supported by the David and Lucile Packard Foundation through the Monterey Bay Aquarium Research Institute. The NSF funded installation and maintenance of the MARS cabled observatory through awards 0739828 and 1114794. W.K.O. was supported by a postdoctoral fellowship from the David and Lucile Packard Foundation through the Monterey Bay Aquarium Research Institute.

## References

1. Abrahms, B. *et al*. Emerging Perspectives on Resource Tracking and Animal Movement Ecology. *Trends Ecol. Evol.* 36, 308–320 (2021).
2. Mueller, T. *et al*. How landscape dynamics link individual- to population-level movement patterns: a multispecies comparison of ungulate relocation data. *Glob. Ecol. Biogeogr.* 20, 683–694 (2011).
3. Mueller, T. & Fagan, W. F. Search and navigation in dynamic environments – from individual behaviors to population distributions. *Oikos* 117, 654–664 (2008).
4. Teitelbaum, C. S. & Mueller, T. Beyond Migration: Causes and Consequences of Nomadic Animal Movements. *Trends Ecol. Evol.* 34, 569–581 (2019).
5. Aikens, E. O. *et al*. The greenscape shapes surfing of resource waves in a large migratory herbivore. *Ecol. Lett.* 20, 741–750 (2017).
6. Armstrong, J. B., Takimoto, G., Schindler, D. E., Hayes, M. M. & Kauffman, M. J. Resource waves: phenological diversity enhances foraging opportunities for mobile consumers. *Ecology* 97, 1099–1112 (2016).
7. Deacy, W. W. *et al*. Phenological tracking associated with increased salmon consumption by brown bears. *Sci. Rep.* 8, 11008 (2018).
8. Middleton, A. D. *et al*. Green-wave surfing increases fat gain in a migratory ungulate. *Oikos* 127, 1060–1068 (2018).
9. Fryxell, J. M. & Sinclair, A. R. E. Causes and consequences of migration by large herbivores. *Trends Ecol. Evol.* 3, 237–241 (1988).

10. Bastille-Rousseau, G. *et al*. Migration triggers in a large herbivore: Galápagos giant tortoises navigating resource gradients on volcanoes. *Ecology* 100, e02658 (2019).
11. Brönmark, C. *et al*. There and back again: migration in freshwater fishes. *Can. J. Zool.* 92, 467–479 (2014).
12. Lok, E. *et al*. Spatiotemporal associations between Pacific herring spawn and surf scoter spring migration: evaluating a 'silver wave' hypothesis. *Mar. Ecol. Prog. Ser.* 457, 139–150 (2012).
13. Block, B. A. *et al*. Tracking apex marine predator movements in a dynamic ocean. *Nature* 475, 86–90 (2011).
14. Boustany, A. M., Matteson, R., Castleton, M., Farwell, C. & Block, B. A. Movements of pacific bluefin tuna (Thunnus orientalis) in the Eastern North Pacific revealed with archival tags. *Prog. Oceanogr.* 86, 94–104 (2010).
15. Oestreich, W. K. *et al*. Acoustic signature reveals blue whales tune life-history transitions to oceanographic conditions. *Funct. Ecol.* 36, 882–895 (2022).
16. Abrahms, B. *et al*. Memory and resource tracking drive blue whale migrations. *Proc. Natl. Acad. Sci. U.S.A.* 116, 5582–5587 (2019).
17. Ryan, J. P. *et al*. Oceanic giants dance to atmospheric rhythms: Ephemeral wind-driven resource tracking by blue whales. *Ecol. Lett.* 25, 2435–2447 (2022).
18. Shuert, C. R. *et al*. Decadal migration phenology of a long-lived Arctic icon keeps pace with climate change. *Proc. Natl. Acad. Sci. U.S.A.* 119, e2121092119 (2022).
19. Robison, B. H. Deep pelagic biology. *J. Exp. Mar. Biol. Ecol.* 300, 253–272 (2004).
20. Messié, M. *et al*. Coastal upwelling drives ecosystem temporal variability from the surface to the abyssal seafloor. *Proc. Natl. Acad. Sci. U.S.A.* 120, e2214567120 (2023).
21. Urmy, S. S., Horne, J. K. & Barbee, D. H. Measuring the vertical distributional variability of pelagic fauna in Monterey Bay. *ICES J. Mar. Sci.* 69, 184–196 (2012).
22. Stewart, J. S. *et al*. Combined climate- and prey-mediated range expansion of Humboldt squid (Dosidicus gigas), a large marine predator in the California Current System. *Glob. Change Biol.* 20, 1832–1843 (2014).
23. Girard, F. *et al*. Phenology in the deep sea: seasonal and tidal feeding rhythms in a keystone octocoral. *Proc. R. Soc. B* 289, 20221033 (2022).
24. Dall'Olmo, G., Dingle, J., Polimene, L., Brewin, R. J. W. & Claustre, H. Substantial energy input to the mesopelagic ecosystem from the seasonal mixed-layer pump. *Nat. Geosci.* 9, 820–823 (2016).
25. Fais, A. *et al*. Sperm whale echolocation behaviour reveals a directed, prior-based search strategy informed by prey distribution. *Behav. Ecol. Sociobiol.* 69, 663–674 (2015).
26. Kawakami, T. A review of sperm whale food. *Sci. Rep. Whales Res. Inst.* 32, 199–218 (1980).
27. Møhl, B., Wahlberg, M., Madsen, P. T., Heerfordt, A. & Lund, A. The monopulsed nature of sperm whale clicks. *J. Acoust. Soc. Am.* 114, 1143–1154 (2003).
28. Solsona-Berga, A., Posdaljian, N., Hildebrand, J. A. & Baumann-Pickering, S. Echolocation repetition rate as a proxy to monitor population structure and dynamics of sperm whales. *Remote Sens. Ecol. Conserv.* 8, 827–840 (2022).
29. Gordon, J. C. D. Evaluation of a method for determining the length of sperm whales (Physeter catodon) from their vocalizations. *J. Zool.* 224, 301–314 (1991).
30. Whitehead. H. *Sperm whales: social evolution in the ocean.* (University of Chicago Press, 2003).
31. Davis, R. *et al*. Diving behavior of sperm whales in relation to behavior of a major prey species, the jumbo squid, in the Gulf of California, Mexico. *Mar. Ecol. Prog. Ser.* 333, 291–302 (2007).
32. Mellinger, D. K., Stafford, K. M. & Fox, C. G. Seasonal occurrence of sperm whale (*Physeter macrocephalus*) sounds in the Gulf of Alaska, 1999–2001. *Mar. Mammal Sci.* 20, 48–62 (2004).

33. Diogou, N. *et al*. Sperm whale (*Physeter macrocephalus*) acoustic ecology at Ocean Station PAPA in the Gulf of Alaska – Part 1: Detectability and seasonality. *Deep Sea Res. 1 Oceanogr. Res. Pap.* 150, 103047 (2019).
34. Straley, J. *et al*. Depredating sperm whales in the Gulf of Alaska: local habitat use and long distance movements across putative population boundaries. *Endanger. Species Res.* 24, 125–135 (2014).
35. Mizroch, S. A. & Rice, D. W. Ocean nomads: Distribution and movements of sperm whales in the North Pacific shown by whaling data and Discovery marks. *Mar. Mammal Sci.* 29, E136–E165 (2013).
36. Mesnick, S. L. *et al*. Sperm whale population structure in the eastern and central North Pacific inferred by the use of single-nucleotide polymorphisms, microsatellites and mitochondrial DNA. *Mol. Ecol. Resour.* 11, 278–298 (2011).
37. Lefort, K. J., Hussey, N. E., Jones, J. M., Johnson, K. F. & Ferguson, S. H. Satellite-tracked sperm whale migrates from the Canadian Arctic to the subtropical western North Atlantic. *Mar. Mammal Sci.* 38, 1242–1248 (2022).
38. Pitman, R. L., Ballance, L. T., Mesnick, S. I. & Chivers, S. J. Killer Whale Predation on Sperm Whales: Observations and Implications. *Mar. Mammal Sci. 17*, 494–507 (2001).
39. Jaquet, N. How spatial and temporal scales influence understanding of Sperm Whale distribution: a review. *Mammal Rev.* 26, 51–65 (1996).
40. Levin, S. A. The Problem of Pattern and Scale in Ecology: The Robert H. MacArthur Award Lecture. *Ecology* 73, 1943–1967 (1992).
41. Oliver, R. Y. *et al*. Eavesdropping on the Arctic: Automated bioacoustics reveal dynamics in songbird breeding phenology. *Sci. Adv.* 4, eaaq1084 (2018).
42. Mellinger, D., Stafford, K., Moore, S., Dziak, R. & Matsumoto, H. An Overview of Fixed Passive Acoustic Observation Methods for Cetaceans. *Oceanography* 20, 36–45 (2007).
43. Oestreich, W. K. *et al*. Animal-Borne Metrics Enable Acoustic Detection of Blue Whale Migration. *Curr. Biol.* 30, 4773-4779.e3 (2020).
44. Morgan, C. A., Beckman, B. R., Weitkamp, L. A. & Fresh, K. L. Recent Ecosystem Disturbance in the Northern California Current. *Fisheries* 44, 465–474 (2019).
45. Walsh, J. E. *et al*. The high latitude marine heat wave of 2016 and its impacts on Alaska. *Bull. Am. Meteorol. Soc.* 99, S39–S43.
46. Diogou, N. *et al*. Sperm whale (Physeter macrocephalus) acoustic ecology at Ocean Station PAPA in the Gulf of Alaska – Part 2: Oceanographic drivers of interannual variability. *Deep Sea Res. 2 Top. Stud. Oceanogr.* 150, 103044 (2019).
47. Merkle, J. A. *et al*. Site fidelity as a maladaptive behavior in the Anthropocene. *Front. Ecol. Environ.* 20, 187–194 (2022).
48. Cavole, L. M. *et al*. Biological Impacts of the 2013–2015 Warm-Water Anomaly in the Northeast Pacific: Winners, Losers, and the Future. *Oceanography* 29, 273–285 (2016).
49. Arranz, P. *et al*. Risso's dolphins plan foraging dives. J. Exp. Biol. 221, jeb165209 (2018).
50. Sato, M. & Benoit-Bird, K. J. Spatial variability of deep scattering layers shapes the Bahamian mesopelagic ecosystem. *Mar. Ecol. Prog. Ser.* 580, 69–82 (2017).
51. Roeleke, M. *et al*. Insectivorous bats form mobile sensory networks to optimize prey localization: The case of the common noctule bat. *Proc. Natl. Acad. Sci. U.S.A.* 119, e2203663119 (2022).
52. Aikens, E. O., Bontekoe, I. D., Blumenstiel, L., Schlicksupp, A. & Flack, A. Viewing animal migration through a social lens. *Trends Ecol. Evol.* 37, 985–996 (2022).
53. Oestreich, W. K. *et al*. The influence of social cues on timing of animal migrations. *Nat. Ecol. Evol.* 6, 1617–1625 (2022).
54. Archibald, K. M., Siegel, D. A. & Doney, S. C. Modeling the Impact of Zooplankton Diel Vertical Migration on the Carbon Export Flux of the Biological Pump. *Glob. Biogeochem. Cycles* 33, 181–199 (2019).
55. Fischer, J. & Visbeck, M. Seasonal variation of the daily zooplankton migration in the Greenland sea. *Deep Sea Res. Part 1 Oceanogr. Res. Pap.* 40, 1547–1557 (1993).

56. Benoit-Bird, K. J. & Lawson, G. L. Ecological Insights from Pelagic Habitats Acquired Using Active Acoustic Techniques. *Annu. Rev. Mar. Sci.* 8, 463–490 (2016).
57. Urmy, S. S. & Benoit-Bird, K. J. Fear dynamically structures the ocean's pelagic zone. *Curr. Biol.* 31, 5086-5092.e3 (2021).
58. Oestreich, W. K., Chapman, M. S. & Crowder, L. B. A comparative analysis of dynamic management in marine and terrestrial systems. *Front. Ecol. Environ.* 18, 496–504 (2020).
59. Maxwell, S. M., Gjerde, K. M., Conners, M. G. & Crowder, L. B. Mobile protected areas for biodiversity on the high seas. *Science* 367, 252–254 (2020).
60. Zhang, Y., McGill, P. R. & Ryan, J. P. Optimized design of windowed-sinc anti-aliasing filters for phase-preserving decimation of hydrophone data. *J. Acoust. Soc. Am.* 151, 2077–2084 (2022).
61. Charif, R. A., Waack, A. M., & Strickman, L. M. Raven Pro 1.4 user's manual. (2010).
62. Wahlberg, M. The acoustic behaviour of diving sperm whales observed with a hydrophone array. *J. Exp. Mar. Biol. Ecol.* 281, 53–62 (2002).
63. Ryan, J. P. et al. Reduction of Low-Frequency Vessel Noise in Monterey Bay National Marine Sanctuary During the COVID-19 Pandemic*. Front. Mar. Sci.* 8, (2021).
64. Zimmer, W. M. X., Tyack, P. L., Johnson, M. P. & Madsen, P. T. Three-dimensional beam pattern of regular sperm whale clicks confirms bent-horn hypothesis. *J. Acoust. Soc. Am.* 117, 1473–1485 (2005).
65. Mathias, D. *et al*. Acoustic and diving behavior of sperm whales (Physeter macrocephalus) during natural and depredation foraging in the Gulf of Alaska. *J. Acoust. Soc. Am.* 132, 518–532 (2012).
66. Chassignet, E. P. *et al*. The HYCOM (hybrid coordinate ocean model) data assimilative system. *J. Mar. Syst.* 65, 60-83 (2007).
67. Collins, M. D. A split-step Padé solution for the parabolic equation method. *J. Acoust. Soc. Am.* 93, 1736–1742 (1993).
68. Abrahms, B. *et al*. Suite of simple metrics reveals common movement syndromes across vertebrate taxa. *Mov. Ecol.* 5, 12 (2017).
69. Moore, J. & Barlow, J. Improved abundance and trend estimates for sperm whales in the eastern North Pacific from Bayesian hierarchical modeling. *Endanger. Species Res.* 25, 141–150 (2014).
70. R Core Team (2022). R: A language and environment for statistical computing. R Foundation for Statistical Computing, Vienna, Austria. https://www.R-project.org/.
71. Vihtakari, M (2022). ggOceanMaps: Plot Data on Oceanographic Maps using 'ggplot2'. R package version 1.3.4. https://CRAN.R-project.org/package=ggOceanMaps.
72. Hijmans, R (2022). geosphere: Spherical Trigonometry. R package version 1.5-18, https://CRAN.R-project.org/package=geosphere.
73. The MathWorks Inc. (2022). MATLAB version: 9.13.0 (R2022b), Natick, Massachusetts: The MathWorks Inc. https://www.mathworks.com.
74. Ryan, J. *et al*. New Passive Acoustic Monitoring in Monterey Bay National Marine Sanctuary. *OCEANS 2016 MTS/IEEE Monterey*, 1-8 (2016).
75. Oestreich, W.K. Data and code for: Acoustic evidence for seasonal resource-tracking migration by a top predator of the deep sea. Zenodo. https://doi.org/10.5281/zenodo.7860426. Deposited April 24, 2023.

## Figures

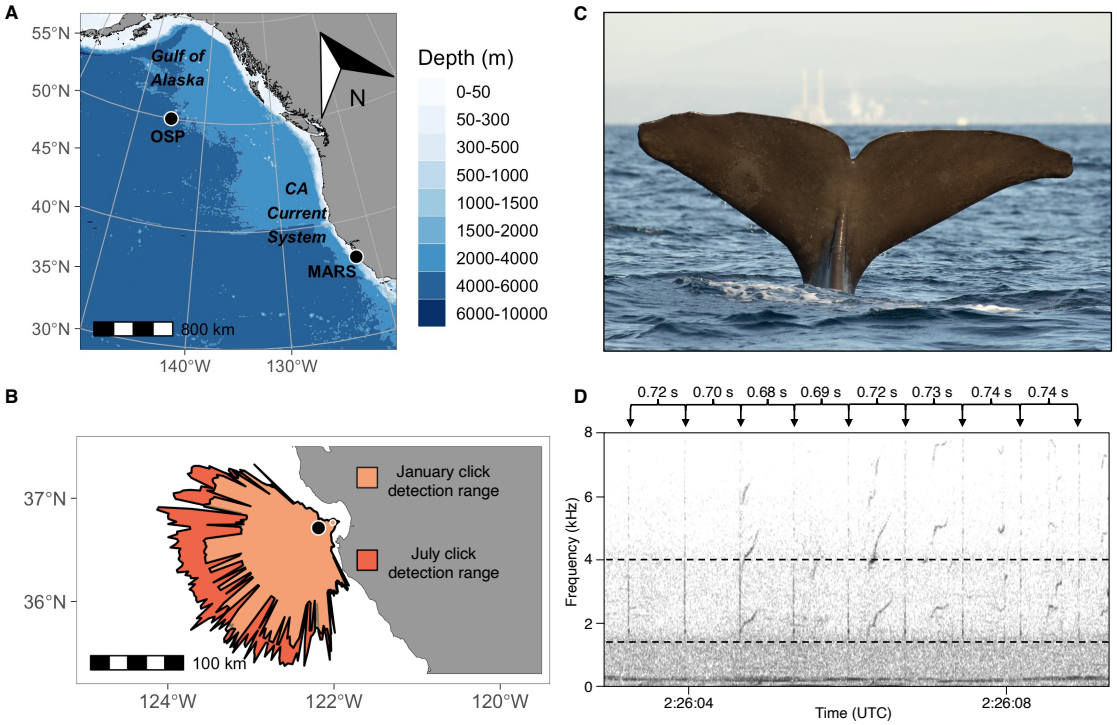


**Figure 1. Study system and methods. (A)** The Northeast Pacific Ocean, showing the location of passive acoustic recordings from the present study (Monterey Accelerated Research System (MARS) in the Central California Current System) and previous studies (32, 33) (Ocean Station PAPA (OSP) in the Gulf of Alaska). **(B)** The Central California Current System, indicating winter and summer detection ranges for sperm whale echolocation clicks produced at 500m depth (see Materials and Methods and SI for additional depths) based on average January and July oceanographic conditions over the period 2016-2022. Larger filled circle indicates MARS (891m depth) and smaller open circle indicates a rare sighting of a sperm whale inshore of this location on Nov 30, 2022 (bottom depth 720m). **(C)** Photograph of one of three individuals sighted at the location noted in panel B, with Moss Landing, California visible in the background (courtesy of Tim Huntington). **(D)** Spectrogram of audio recorded at MARS during the sighting in panels B-C, showing a period when a single foraging sperm whale's echolocation clicks (impulsive, broadband signals) were clearly visible and audible. Dashed horizontal lines indicate the minimum and maximum frequencies of the automated energy detector used to detect sperm whale echolocation clicks. Note the near-constant inter-click-interval used to discern echolocating sperm whales from other impulsive sound sources in this frequency range (see Materials and Methods for details).

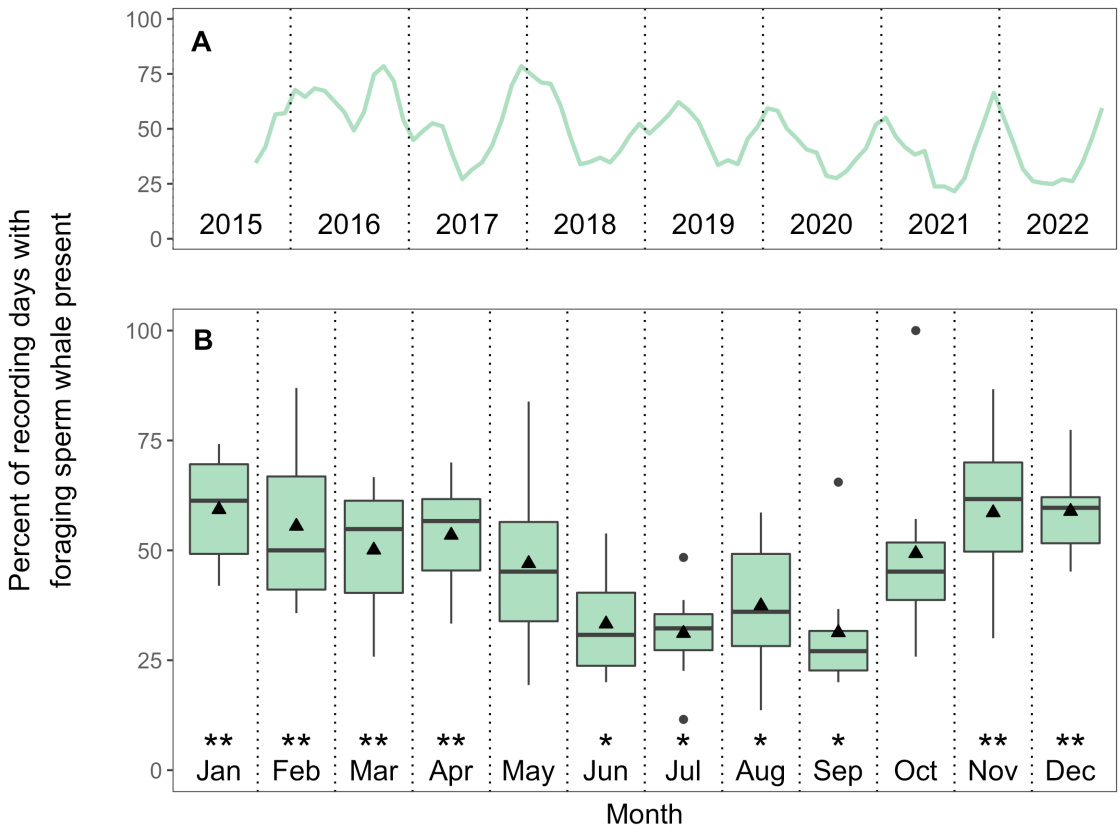


**Figure 2. Variability in foraging sperm whale presence. (A)** Monthly percent presence over the full study period (smoothed with a 3-month running mean). **(B)** Annual cycle of echolocating sperm whale presence over the full study period (Aug 2015 – Dec 2022). Boxplots show the median (center line), mean (triangle), 25$^{th}$-75$^{th}$ percentile (box), ± 1.5*IQR (whiskers), and outlying points. *Indicates statistically-significant difference in mean relative to the maximum month (January). **Indicates statistically-significant difference in mean relative to the minimum month (July). See Figure S2 for additional statistical assessment of seasonality.

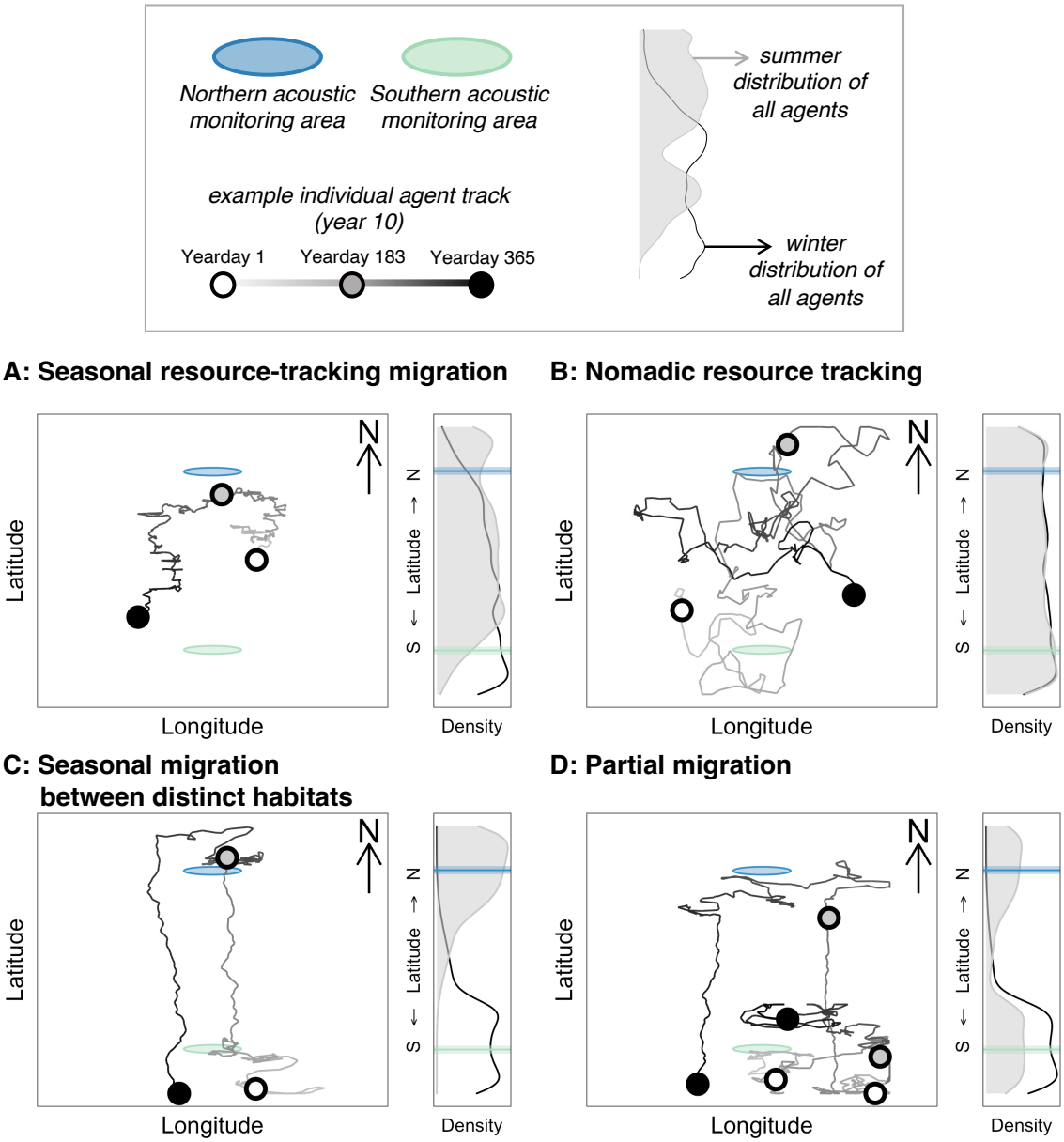


**Figure 3. Simulated individual-level movement strategies.** Top panel provides a legend for simulation results. In each of the bottom panels A-D, one individual agent's track (two agents in the case of partial migration) is shown from year 10 of the simulation alongside the summer and winter distribution of all agents over years 2-10. Circular acoustic monitoring areas appear elliptical due to distortion of the simulation domain in this visualization to highlight individual agent tracks. **(A)** Seasonal resource-tracking migration. **(B)** Nomadic resource tracking. **(C)** Seasonal migration between distinct habitats. **(D)** Partial migration, showing one migratory and one resident individual track.

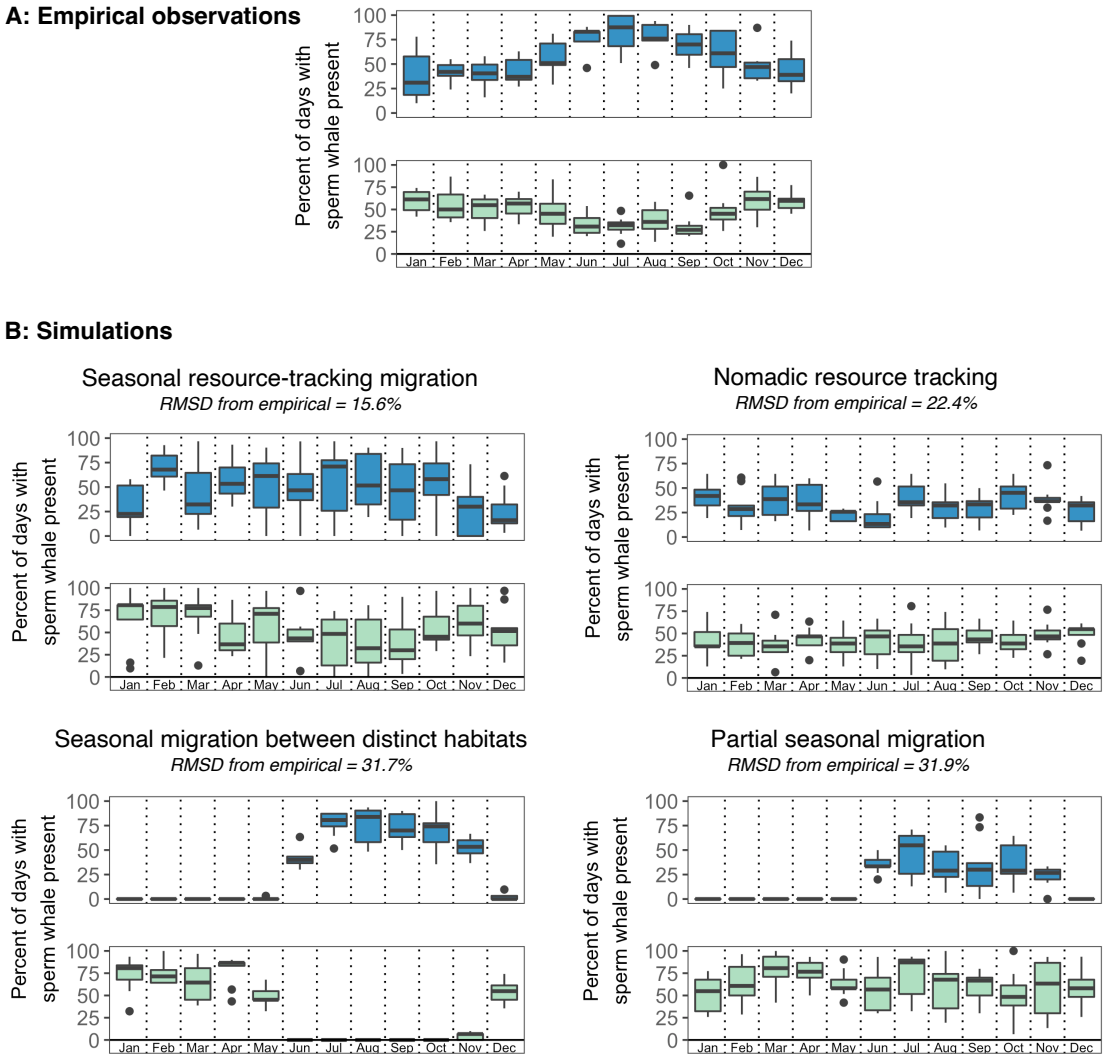


**Figure 4. Comparison of empirical and simulated acoustic detection seasonality under different hypothesized individual-level movement strategies. (A)** Empirical acoustic detections from the Central California Current System (green; present study) and the Gulf of Alaska (blue; (32, 33)). **(B)** Acoustic detection at northern (blue) and southern (green) listening ranges for simulated agents following each of the hypothesized movement strategies. Boxplots show the median (center line), 25$^{th}$-75$^{th}$ percentile (box), ± 1.5*IQR (whiskers), and outlying points of monthly acoustic detection over years 2-10 of each simulation. RMSD refers to the root-mean-square deviation of each simulation's monthly mean acoustic detection results relative to empirical observations.

## Supporting Information for

# Acoustic evidence for seasonal resource-tracking migration by a top predator of the deep sea

William K. Oestreich[a,*], Kelly J. Benoit-Bird[a], Briana Abrahms[b], Tetyana Margolina[c], John E. Joseph[c], Yanwu Zhang[a], Carlos A. Rueda[a], John P. Ryan[a]

*Corresponding author: William K. Oestreich

Email: woestreich.research@gmail.com

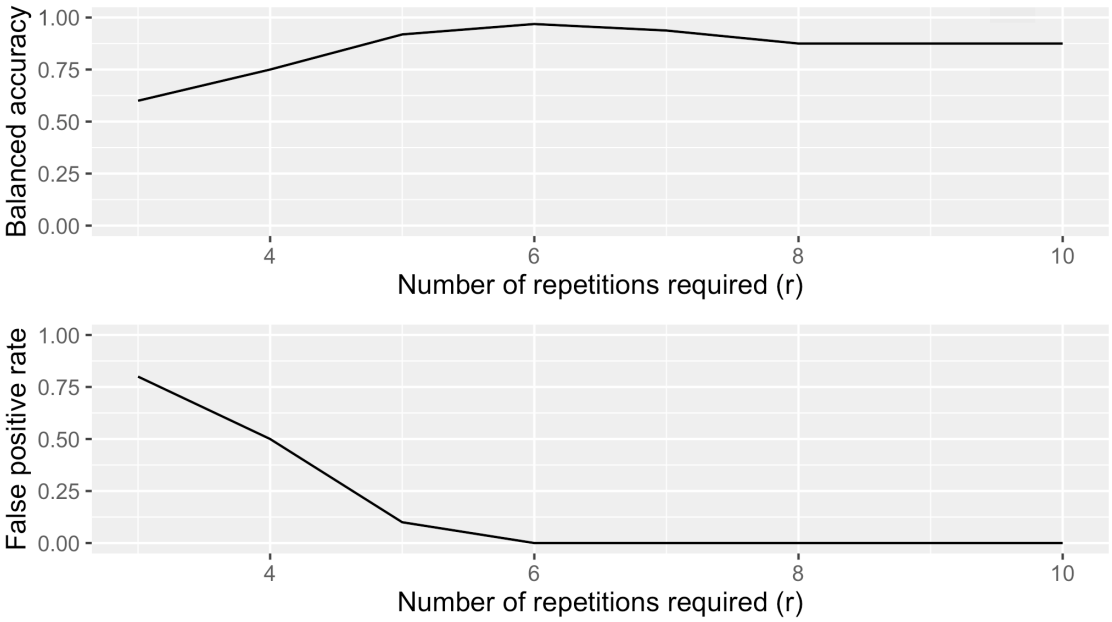


**Fig. S1.** Performance of automated daily acoustic processing relative to manual assessment. Requiring six repetitions of click detection at near-constant inter-click interval (r = 6) yields a daily balanced accuracy of 97% and daily false positive rate of 0%.

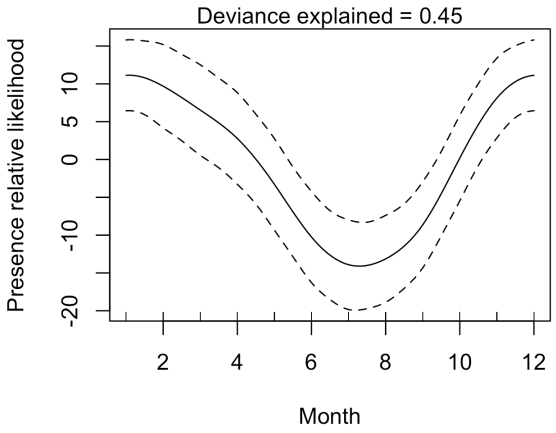


**Fig. S2.** Seasonal generalized additive model fit relationship.

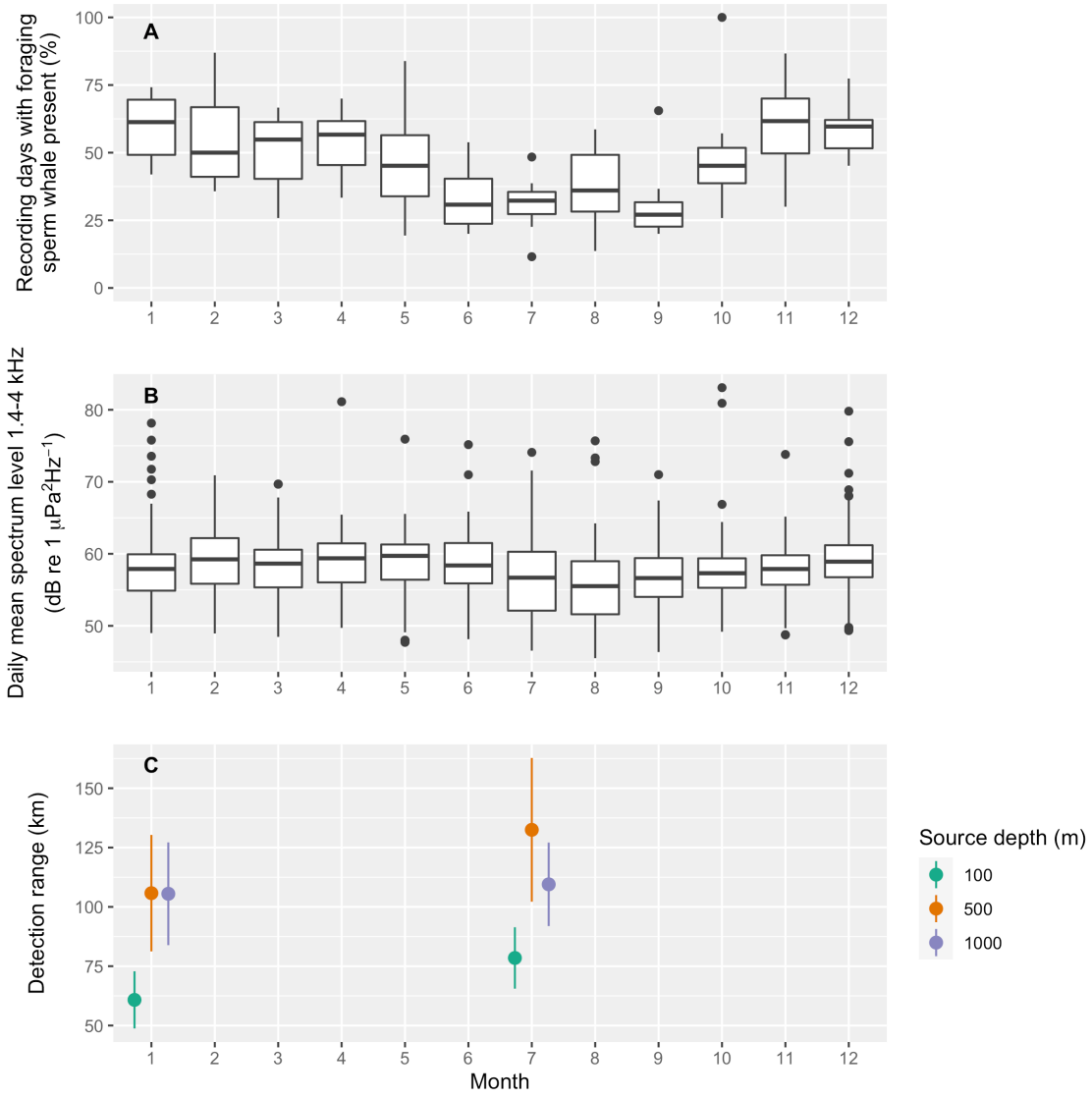


**Fig. S3. Seasonal variation in listening conditions at MARS. (A)** Average annual cycle of echolocating sperm whale presence averaged over the full study period (Aug 2015 – Dec 2022), reproduced from Figure 2B in the main text. **(B)** Average annual cycle of ambient noise conditions at MARS in the frequency range (1.4-4kHz) targeted by the band limited energy detector employed to identify candidate sperm whale echolocation detections. **(C)** Estimated maximum detection range at MARS for sperm whale echolocation clicks produced at depths of 100, 500, and 1000m during the maximum (January) and minimum (July) months of foraging sperm whale presence. Points and lines represent the mean and standard deviation of 1-degree bearing ranges between 154-311° around MARS, representing the offshore area where 500m and 1000m source depth results are not limited by the shelf break (Figure 1B), and where sperm whales are most likely to be found. See Materials and Methods for information on modeling of acoustic propagation and detection range.

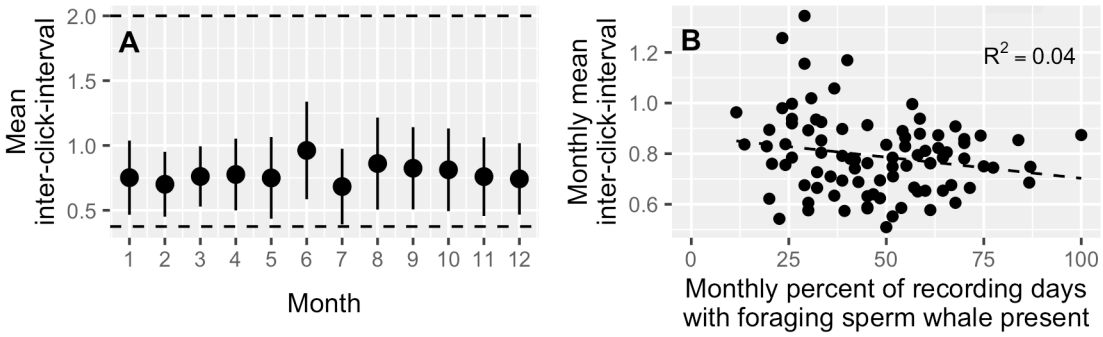


**Fig. S4. Inter-click-interval (ICI) comparisons. (A)** Average annual cycle of monthly mean ICI, showing means (points) and standard deviations (lines). Dashed horizontal lines indicate the maximum and minimum ICIs for automated click detection. **(B)** Monthly mean ICI vs. monthly percent presence, indicating no significant relationship between these variables ($p > 0.05$).

**Table S1.** Band limited energy detector parameters.

| | |
|---|---|
| **BLED signal calculation** | |
| Min. Frequency | 1.4 kHz |
| Max. Frequency | 4.0 kHz |
| Min. Duration | 8.125 ms |
| Max. Duration | 32.5 ms |
| Min. Separation | 32.5 ms |
| **BLED noise calculation** | |
| Block size | 2.0 s |
| Hop size | 0.5 s |
| Percentile | 20.0 |
| **Signal-to-noise parameters** | |
| Min. Occupancy | 70.0% |
| SNR Threshold | 5.0 dB |
| **Spectrogram calculation** | |
| Window | Hann |
| Window Size | 512 samples |
| Window Overlap | 95% |